Asociación Argentina
de Mecánica Computacional

Mecánica Computacional Vol XXXII, págs. 2131-2152 (artículo completo)
Carlos G. García Garino, Aníbal E. Mirasso, Mario A. Storti, Miguel E. Tornello (Eds.)
Mendoza, Argentina, 19-22 Noviembre 2013

VIBRATION ANALYSIS OF AXIALLY FUNCTIONALLY GRADED ROTATING TIMOSHENKO BEAMS WITH GENERAL VARIATION OF CROSS SECTION, WITH DQM AND FEM

Daniel H. Felix[a], **Diana V. Bambill**[a, b], **Carlos A. Rossit**[a, b] **and Julian Reta**[a]

[a]*Departamento de Ingeniería, Instituto de Mecánica Aplicada, Universidad Nacional del Sur, Av. Alem 1253, Bahía Blanca, Argentina, dhfelix@uns.edu.ar*

[b]*CONICET, Bahía Blanca, Argentina, dvbambill@criba.edu.ar*

Keywords: functionally graded materials, rotating beam, Timoshenko, free vibration.

Abstract. A new approach to study transversal vibration of rotating Timoshenko beams is presented. It is an extension of previous works that consider the simultaneous presence of axially functionally graded materials, and variation of the cross section. The quadrature algorithms extensions were developed by the authors. The model in analysis includes a lot of important features like effects of material non-homogeneity, shear deformation, rotatory inertia, centrifugal stiffening action, gyroscopic effects, and stepped variation of the cross section. The numerical study is implemented using the differential quadrature method and the results are compared with values obtained from particular cases available in the literature, when it is possible. Since a lot of characteristics are considered, it is a very versatile model which is solved with an efficient method. It is hoped that both, the numerical study carried out and the proposed algorithms provide useful information that will be of scientific and technological interest.

1 INTRODUCTION

In the present work is extended the develop of a particular methodology that solves the rotating Timoshenko beam Lin and Hsiao (2001), taking into account a large number of parameters in the model. Among these features, the relevant characteristic in the present approach, is the consideration of axially functionally graded materials properties. The axially functionally graded materials, (AFGM), are becoming as a good alternative to overcome the principal disadvantages presented in composite materials, such as residual stress, locally plastic deformation, debonding between adjacent surfaces of different materials and so on, as have been remarked by Yaghoobi and Fereidoon (2010). In the case of helicopter blades, wind turbine blades, or ship propellers between others, the mentioned advantages has generated renewed efforts to investigate the dynamic properties of structural elements made with AFGM, Rajasekaran (2012).

Due the fact the system under study contains many parameters, a large variety of beam models are possible. Accordingly, the numerical simulation of these models becomes necessary, primarily because cover all cases with experimental studies would be too costly. Furthermore, the desired good precision of the results, requires the use of effective methods to solve the corresponding governing differential equations. Among these methods, are frequently applied for this purpose, the finite element method Przemieniecki (1968); Petyt (1990); Rossi (2007), the dynamic stiffness formulation Banerjee (2000, 2001); Banerjee et al. (2006) and the differential quadrature method Bellman and Casti (1971); Bert and Malik (1996); Shu and Chen (1999); Karami et al. (2003).

In the present approach, are extended the develop of algorithms based on generalized differential quadrature method with domain decomposition technique, to be applied at rotating beams, made with non homogeneous materials Felix et al. (2008, 2009); Bambill et al. (2010). The work begins describing the principal characteristics and parameters of the beams under analysis. Then, the governing equations are developed in detail, including the corresponding non-dimensional expressions. With these expressions, the quadrature analogous differential equations, necessary to apply the differential quadrature method, are obtained. In the numerical results section, a set of different beam models with different boundary conditions are analized. Some of the calculated results are compared with values obtained from the available technique literature.

2 GEOMETRICAL AND MECHANICAL PROPERTIES

The proposed model is constituted by a set of beam-parts which are refered as k elements. So, the integer k is simply a beam element identifier. In general, each of the k elements may have different geometrical and mechanical properties. Moreover, to carry out the present dynamical study, the system is analyzed with the rotating Timoshenko beam theory, which include shear deformation, rotatory inertia and the effects of centrifugal forces, Banerjee (2000, 2001). The geometry of the models under study is shown in Figure 1 for the particular case of the beam composed by 2 elements.

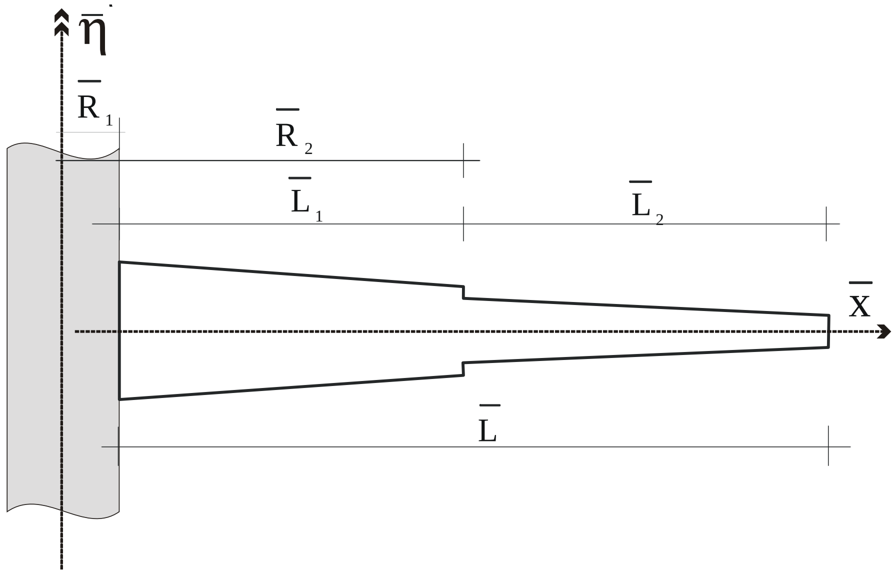

Figure 1: Geometry of the beam composed by 2 elements.

In Figure 1, $\overline{L}_1$ and $\overline{L}_2$ are the length of each element and $\overline{L}$ is the total length of the beam. $\overline{\eta}$ represents the angular velocity of the beam, and $\overline{W}$ is the corresponding transversal deflection of the beam when it does experiment transversal vibration. Notice that in this particular case under study the radius hub was adopted equal to zero.

In Figure 2, it is shown a k element with their principal geometric variables.

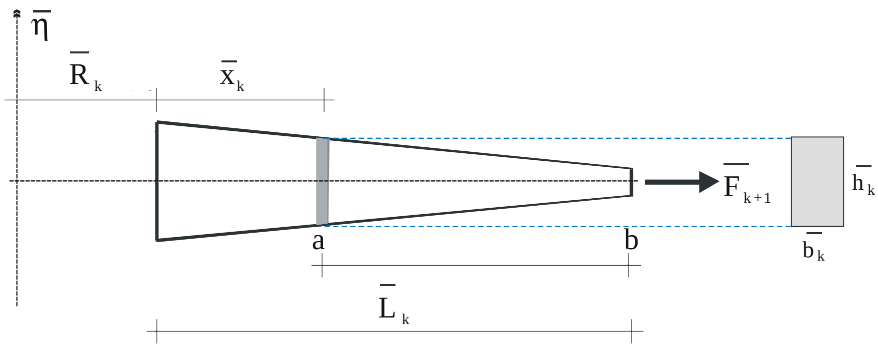

Figure 2: Geometry of the k element along the x-axis.

2.1 Spatial coordinates

In Figure 2, $\overline{R}_k$ is the spatial coordinate at the beginning of each k element and $\overline{x}_k$ is the spatial coordinate which locate any cross section within the corresponding k element.

For simplicity, in Figure 2, only a k element is shown. The rectangular cross section, adopted in the present work, is defined by $\overline{b}_k(\overline{x}_k)$ and $\overline{h}_k(\overline{x}_k)$. As it is obvious, at the beginning of each k element $\overline{x}_k = 0$ and the variables a and b, represent the integral ends in the expression of centrifugal forces, that will be defined later. The non-dimensional spatial coordinate is defined as follow:

$$x = \frac{\overline{x}_k}{\overline{L}_k}, \tag{1}$$

where $\overline{L}_k$ is the length of each k element. Notice that the non-dimensional coordinate x do not depend of k. The non-dimensional length of each k element will be:

$$L_k = \frac{\overline{L}_k}{\overline{L}}. \tag{2}$$

2.2 Material properties

Axially functionally graded beams represent a particular application of AFGM, widely used in mechanical and aeronautical engineering. It is assumed that each k element of the beam is composed of two materials named $material_{Ak}$ and $material_{Bk}$. The corresponding Young modulus will be $\overline{E}_{Ak}$ and $\overline{E}_{Bk}$ and the corresponding mass density will be $\overline{\rho}_{Ak}$ and $\overline{\rho}_{Bk}$. The aspect ratio of the two mentioned materials for Young modulus and for density, are defined as follow:

$$\chi_{E_k} = \frac{\overline{E}_{Bk}}{\overline{E}_{Ak}}; \qquad \text{with} \qquad \overline{E}_{Ak} > \overline{E}_{Bk}, \tag{3}$$

similarly for the density it gives:

$$\chi_{\rho_k} = \frac{\overline{\rho}_{Bk}}{\overline{\rho}_{Ak}}; \qquad \text{with} \qquad \overline{\rho}_{Ak} > \overline{\rho}_{Bk}. \tag{4}$$

Following a power law distribution, the Young modulus is expressed as:

$$\overline{E}_k(\overline{x}_k) = \overline{E}_{Ak}\left((\chi_{E_k} - 1)(\frac{\overline{x}_k}{\overline{L}_k})^{n_{Ek}} + 1\right). \tag{5}$$

Introducing the non-dimensional spatial coordinate (1) in equation (5), it yields:

$$\overline{E}_k(x) = \overline{E}_{Ak}\left((\chi_{E_k} - 1)x^{n_{Ek}} + 1\right), \tag{6}$$

where n_{E_k} is the exponential parameter that define the variation law of $E_k(x)$ within the k element. The expression of density is:

$$\overline{\rho}_k(\overline{x}_k) = \overline{\rho}_{Ak}\left((\chi_{\rho_k} - 1)(\frac{\overline{x}_k}{\overline{L}_k})^{n_{\rho k}} + 1\right), \tag{7}$$

or:

$$\overline{\rho}_k(x) = \overline{\rho}_{Ak}\left((\chi_{\rho_k} - 1)x^{n_{\rho k}} + 1\right), \tag{8}$$

where n_{ρ_k} is the exponential parameter that define the variation law of $\rho_k(x)$ within the k element.

Next, are defined the non-dimensional expressions of $\overline{E}_k(x)$ and $\overline{\rho}_k(x)$ as follow:

$$E_k(x) = \frac{\overline{E}_k(x)}{\overline{E}_{Ak}} = (\chi_{E_k} - 1)x^{n_{Ek}} + 1, \tag{9}$$

and

$$\rho_k(x) = \frac{\overline{\rho}_k(x)}{\overline{\rho}_{Ak}} = (\chi_{\rho_k} - 1)x^{n_{\rho k}} + 1. \tag{10}$$

The Figures 3 and 4 are the parametric plots of $E_k(x)$, for both, lineal and quadratic variation law. The discontinuous of E and ρ, between adjacent k elements, are taking into account with the following parameters:

$$\alpha_{Ek} = \frac{\overline{E}_k(0)}{\overline{E}_1(0)} = \frac{\overline{E}_{Ak}}{\overline{E}_{A1}}; \qquad \alpha_{\rho k} = \frac{\overline{\rho}_k(0)}{\overline{\rho}_1(0)} = \frac{\overline{\rho}_{Ak}}{\overline{\rho}_{A1}}. \tag{11}$$

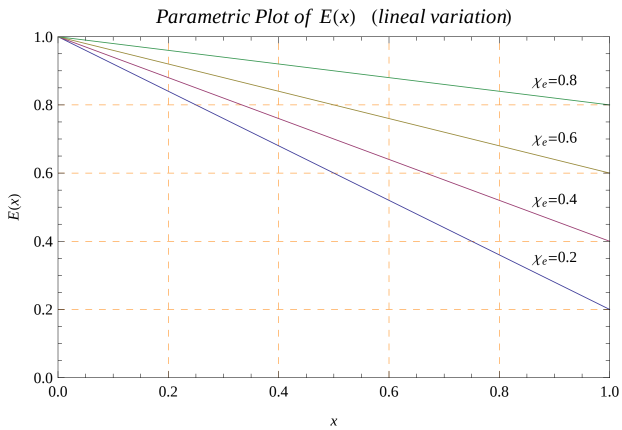

Figure 3: Fundamental frecuency coeficient vs. χ_E and χ_ρ

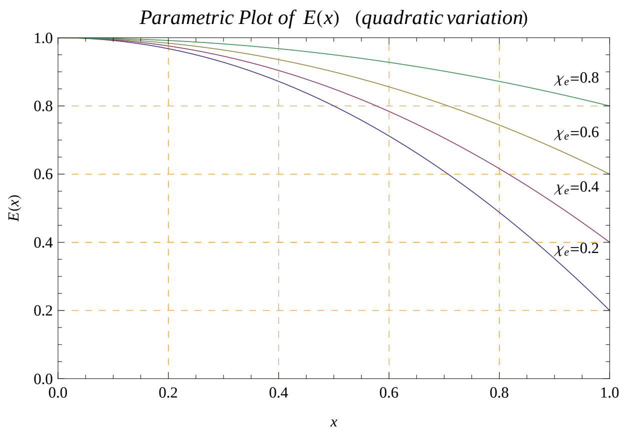

Figure 4: Fundamental frecuency coeficient vs. χ_E and χ_ρ

The plots of $\rho_k(x)$ are not shown because these are similarly to $E_k(x)$.

2.3 Geometrical properties of cross section

The following expressions define the aspect ratio between the heights and between the widths, at both ends of the k element in consideration.

$$\chi_{hk} = \frac{\overline{h}_{Bk}}{\overline{h}_{Ak}}; \qquad \chi_{bk} = \frac{\overline{b}_{Bk}}{\overline{b}_{Ak}}, \tag{12}$$

where $\overline{h}_{Ak}$ and $\overline{b}_{Ak}$ are the height and the width of the beam at the beginning of each k element, respectively. Similarly, $\overline{h}_{Bk}$ and $\overline{b}_{Bk}$ are the height and the width of the beam at the end of each k element, respectively. Following a power law distribution, it is assumed that the height and the width of the cross section in each k element, vary according with the following expressions:

$$\overline{h}_k(\overline{x}_k) = \overline{h}_{Ak}\left((\chi_{hk} - 1)(\frac{\overline{x}_k}{\overline{L}_k})^{n_{hk}} + 1\right), \tag{13}$$

or:

$$\overline{h}_k(x) = \overline{h}_{Ak}\left((\chi_{hk} - 1)x^{n_{hk}} + 1\right), \tag{14}$$

where n_{hk} is the exponential parameter that define the variation law of $\overline{h}_k(x)$ in the k element and:

$$\overline{b}_k(\overline{x}_k) = \overline{b}_{Ak}\left((\chi_{bk} - 1)(\frac{\overline{x}_k}{\overline{L}_k})^{n_{bk}} + 1\right), \tag{15}$$

or:

$$\overline{b}_k(x) = \overline{b}_{Ak}\left((\chi_{bk} - 1)x^{n_{bk}} + 1\right). \tag{16}$$

where n_{bk} is the exponential parameter that define the variation law of $\overline{b}_k(x)$ in the k element. Next, it is defined the non-dimensional expressions of $\overline{h}_k(x)$ and $\overline{b}_k(x)$ as follow:

$$h_k(x) = \frac{\overline{h}_k(x)}{\overline{h}_{Ak}} = (\chi_{hk} - 1)x^{n_{hk}} + 1, \tag{17}$$

and:

$$b_k(x) = \frac{\overline{b}_k(x)}{\overline{b}_{Ak}} = (\chi_{bk} - 1)x^{n_{bk}} + 1. \tag{18}$$

For rectangular cross section, it is obtained the expression of the area from expression (19), using the equations (13) and (15)

$$\overline{A}_k(\overline{x}_k) = \overline{b}_k(\overline{x}_k)\overline{h}_k(\overline{x}_k), \tag{19}$$

or:

$$\overline{A}_k(x) = \overline{b}_k(x)\overline{h}_k(x). \tag{20}$$

Then, the non-dimensional expression of $\overline{A}_k(x)$ result:

$$A_k(x) = \frac{\overline{A}_k(x)}{\overline{b}_{Ak}\overline{h}_{Ak}} = \frac{\overline{A}_k(x)}{\overline{A}_k(0)} = b_k(x)h_k(x). \tag{21}$$

Similarly, it is obtained the inertia moment of the cross section within the k element, as follow:

$$\overline{I}_k(\overline{x}_k) = \frac{1}{12}\overline{b}_k(\overline{x}_k)\overline{h}_k(\overline{x}_k)^3, \tag{22}$$

or:

$$\overline{I}_k(x) = \frac{1}{12}\overline{b}_k(x)\overline{h}_k(x)^3, \tag{23}$$

and the corresponding non-dimensional expression of $I_k(x)$ result:

$$I_k(x) = \frac{12}{\overline{b}_{Ak}\overline{h}_{Ak}^3}\overline{I}_k(x) = \frac{\overline{I}_k(x)}{\overline{I}_k(0)} = b_k(x)h_k(x)^3. \tag{24}$$

For discontinuous variation of $\overline{A}$ and $\overline{I}$ between adjacent k elements are defined the following parameters:

$$\alpha_{Ak} = \frac{\overline{A}_k(0)}{\overline{A}_1(0)}; \qquad \alpha_{Ik} = \frac{\overline{I}_k(0)}{\overline{I}_1(0)}. \tag{25}$$

3 MATHEMATICAL DEVELOPMENT

To obtain the natural frequencies and mode shapes of the rotating Timoshenko beams it is used the Differential Quadrature Method Bellman and Casti (1971); Bert and Malik (1996); Felix et al. (2008) with domain decomposition technique.

3.1 Dimensional expressions of governing differential equations

The centrifugal force experimented by a differential element, located in the k element of the rotating beam, can be expressed in the form:

$$d\overline{N}_k(\overline{x}_k) = \overline{\eta}^2(\overline{R}_k + \overline{x}_k)\overline{dm}_k(\overline{x}_k), \tag{26}$$

where $\overline{\eta}^2$ is the angular velocity of the beam, $\overline{R}_k$ is the spatial coordinate at the beginning of the k element, $\overline{x}_k$, the spatial coordinate of the element and dm_k the mass element within the k element, which is expressed as follow:

$$\overline{dm}_k(\overline{x}_k) = \overline{\rho}(\overline{x}_k)\overline{A}(\overline{x}_k)d\overline{x}_k, \tag{27}$$

where $\overline{\rho}(\overline{x}_k)$ is the mass density and $\overline{A}(\overline{x}_k)$ the cross section area of the beam at position $\overline{x}_k$. Then, the elemental contribution to the normal force is:

$$d\overline{N}_k(\overline{x}_k) = \overline{\eta}^2(\overline{R}_k + \overline{x}_k)\rho(\overline{x}_k)\overline{A}(\overline{x}_k)d\overline{x}_k. \tag{28}$$

Integrating along the beam it is reached:

$$\overline{N}_k(\overline{x}_k) = \overline{\eta}^2 \left(\overline{R}_k \int_{\overline{x}_k}^{\overline{L}_k} \overline{\rho}_k(\overline{x}_k)\overline{A}_k(\overline{x}_k)d\overline{x}_k + \int_{\overline{x}_k}^{\overline{L}_k} \overline{\rho}_k(\overline{x}_k)\overline{A}_k(\overline{x}_k)\overline{x}_k d\overline{x}_k \right) + \overline{N}_{k+1}, \tag{29}$$

being $\overline{N}_{k+1}$, the centrifugal force at the end of the k element. Making use of the following definitions:

$$\overline{V}_k(\overline{x}_k) = \int_0^{\overline{x}_k} \overline{\rho}_k(\overline{x}_k)\overline{A}_k(\overline{x}_k)d\overline{x}_k, \tag{30}$$

and:

$$\overline{\phi}_k(\overline{x}_k) = \int_0^{\overline{x}_k} \overline{\rho}_k(\overline{x}_k)\overline{A}_k(\overline{x}_k)\overline{x}_k d\overline{x}_k, \tag{31}$$

the equation (29) becomes more compactly, resulting:

$$\overline{N}_k(\overline{x}_k) = \overline{\eta}^2 \left(\overline{R}_k\,\overline{V}_k(L_k) + \overline{\phi}_k(L_k) - \overline{R}_k\,\overline{V}_k(\overline{x}_k) - \overline{\phi}_k(\overline{x}_k)\right) + \overline{N}_{k+1}. \tag{32}$$

In the present approach, it is assumed that the rotating beam is subjected to transverse vibrations harmonically varying in time. Then, the deflection of the beam is given by the expression:

$$\overline{w}_k(\overline{x}_k, t) = \overline{W}_k(\overline{x}_k)cos(\omega t), \tag{33}$$

where $\overline{W}_k(\overline{x}_k)$ is the transversal deflection amplitude of the beam and ω are the corresponding natural frequencies. From application of Hamilton's principle, and after separating variables, it is possible to obtain the expressions of the amplitude of internal forces $\overline{Q}_k(\overline{x}_k)$ and $\overline{M}_k(\overline{x}_k)$ in each k element of the beam Felix et al. (2008). The expression of $\overline{Q}_k(\overline{x}_k)$ is:

$$\overline{Q}_k(\overline{x}_k) = \overline{N}_k(\overline{x}_k)\frac{d\overline{W}_k}{d\overline{x}_k} + \kappa\overline{G}_k(\overline{x}_k)\overline{A}_k(\overline{x}_k)\overline{\gamma}_k(\overline{x}_k), \tag{34}$$

where $\overline{W}_k$ and $d\overline{W}_k/d\overline{x}_k$ are the displacement and the slope amplitude, for the transversal vibration of the beam in the k element respectively. The parameter κ is the shear factor, while $\overline{G}_k(\overline{x}_k)$ is the shear modulus and $\overline{\gamma}_k(\overline{x}_k)$ is the distortion at the $\overline{x}_k$ position, all of them within the k element. The distortion can be expressed in the form:

$$\overline{\gamma}_k(\overline{x}_k) = \frac{d\overline{W}_k}{d\overline{x}_k} - \overline{\Psi}_k, \tag{35}$$

where $\overline{\Psi}_k(\overline{x}_k)$ is the rotation of the cross section in the position $\overline{x}_k$ of the k element. The shear module $\overline{G}_k(\overline{x}_k)$ can be expressed as follow:

$$\overline{G}_k(\overline{x}_k) = \frac{\kappa}{2(1+\nu)}\overline{E}_k(\overline{x}_k), \tag{36}$$

where, as it was defined earlier, $\overline{E}_k(\overline{x}_k)$ is the Young module in the k element. Replacing the expressions (35) and (36) in equation (34) and rearranging terms it is obtained:

$$\begin{aligned}\overline{Q}_k(\overline{x}_k) = \left(\overline{N}_k(\overline{x}_k) + \frac{\kappa}{2(1+\nu)}\overline{E}_k(\overline{x}_k))\overline{A}_k(\overline{x}_k)\right)\frac{d\overline{W}_k}{d\overline{x}_k} - \\ \frac{\kappa}{2(1+\nu)}\overline{E}_k(\overline{x}_k))\overline{A}_k(\overline{x}_k)\overline{\Psi}_k.\end{aligned} \tag{37}$$

The expression of $\overline{M}_k(\overline{x}_k)$ result:

$$\overline{M}_k(\overline{x}_k) = \overline{E}_k(\overline{x}_k)\overline{I}_k(\overline{x}_k)\frac{d\overline{\Psi}_k}{d\overline{x}_k}, \tag{38}$$

where $\overline{W}_k$ and $\overline{\Psi}_k$ are the displacement and rotation amplitude respectively, for the transversal vibration of the beam in the k element, κ is the shear factor. while $\overline{I}_k(\overline{x}_k)$ represents the inertia moment of the cross section.

Once known the internal forces, they can be obtained the governing differential equations of the system from the application of Hamilton principle, Banerjee (2000, 2001). The resulting expressions are showed in equations (39) and (40):

$$-\frac{d\overline{Q}_k(\overline{x}_k)}{d\overline{x}_k} = \overline{\rho}(\overline{x}_k)\overline{A}(\overline{x}_k)\omega^2\overline{W}_k, \tag{39}$$

and:

$$-\overline{Q}_k(\overline{x}_k) + \overline{N}_k(\overline{x}_k)\frac{d\overline{W}_k}{d\overline{x}_k} - \frac{d\overline{M}_k(\overline{x}_k)}{d\overline{x}_k} - \overline{\rho}(\overline{x}_k)\overline{I}(\overline{x}_k)\overline{\eta}^2\overline{\Psi}_k = \overline{\rho}(\overline{x}_k)\overline{I}(\overline{x}_k)\omega^2\overline{\Psi}_k. \tag{40}$$

When the beam is made with more than an element, the compatibility equations are required in the sections that join adjacent elements. The compatibility equations for displacements can be expressed as follow:

$$-\overline{W}_{k-1}|_{\overline{x}_{k-1}=\overline{L}_{k-1}} + \overline{W}_k|_{\overline{x}_k=0} = 0, \tag{41}$$

and:

$$-\overline{\Psi}_{k-1}|_{\overline{x}_{k-1}=\overline{L}_{k-1}} + \overline{\Psi}_k|_{\overline{x}_k=0} = 0. \tag{42}$$

The compatibility equations for internal forces can be expressed in the form:

$$-\overline{Q}_{k-1}|_{\overline{x}_{k-1}=\overline{L}_{k-1}} + \overline{Q}_k|_{\overline{x}_k=0} = 0, \tag{43}$$

and:

$$-\overline{M}_{k-1}|_{\overline{x}_{k-1}=\overline{L}_{k-1}} + \overline{M}_k|_{\overline{x}_k=0} = 0. \tag{44}$$

The following particular cases of boundary conditions for the rotating beam model are considered: Clamped-free, clamped-slider and clamped-clamped.

In the case of clamped-free boundary conditions, geometric boundary restrictions at left end and natural boundary conditions at right end, are imposed:

$$\overline{W}_1|_{\overline{x}_1=0} = 0; \qquad \overline{\Psi}_1|_{\overline{x}_1=0} = 0; \qquad \overline{Q}_d|_{\overline{x}_d=\overline{L}_d} = 0; \qquad \overline{M}_d|_{\overline{x}_d=\overline{L}_d} = 0. \tag{45}$$

In the case of clamped-slider boundary conditions, geometric boundary restrictions at left end and both, geometric and natural boundary conditions at right end, are imposed:

$$\overline{W}_1|_{\overline{x}_1=0} = 0; \qquad \overline{\Psi}_1|_{\overline{x}_1=0} = 0; \qquad \overline{W}_d|_{\overline{x}_d=L_d} = 0; \qquad \overline{M}_d|_{\overline{x}_d=L_d} = 0. \tag{46}$$

Finally, in the case of clamped-clamped boundary conditions, geometric boundary restrictions at both ends are imposed:

$$\overline{W}_1|_{\overline{x}_1=0} = 0; \qquad \overline{\Psi}_1|_{\overline{x}_1=0} = 0; \qquad \overline{W}_d|_{\overline{x}_d=L_d} = 0; \qquad \overline{\Psi}_d|_{\overline{x}_d=L_d} = 0. \tag{47}$$

3.2 Non-dimensional expressions of governing differential equations

Previously to get the quadrature analogous differential equations, it is needed to obtain the corresponding non-dimensional expressions. The non-dimensional expressions corresponding to internal forces are obtained from equations (32), (37) and (38), and are expressed as follow:

$$N_k(x) = \eta^2 \frac{l_k^2}{s_1^2}\left(R_k v_k(1) + \phi_k(1) - R_k v_k(x) - \phi_k(x)\right) + N_{k+1}, \tag{48}$$

where:

$$\eta = \sqrt{\frac{\overline{\rho}_1(0)\overline{A}_1(0)}{\overline{E}_1(0)\overline{I}_1(0)}} L^2 \overline{\eta}, \tag{49}$$

is the non-dimensional expression for rotating velocity of the beam and:

$$s_1 = \frac{L}{i_1}; \qquad i_1 = \sqrt{\frac{I_1(0)}{A_1(0)}}; \qquad R_k = \frac{\overline{R}_k}{L}, \tag{50}$$

are non dimensional parameters for slenderness, turning radius and position, at the beginning of the k element and:

$$v_k(x) = \frac{V_k(\overline{x}_k)}{\overline{L}_k \overline{\rho}_k(0) \overline{A}_k(0)}; \quad \phi_k(x) = \frac{\Phi_k(\overline{x}_k)}{\overline{L}_k^2 \overline{\rho}_k(0) \overline{A}_k(0)}; \quad N_{k+1} = \frac{\overline{N}_{k+1}}{\overline{E}_k(0) \overline{A}_k(0)}, \tag{51}$$

are non dimensional parameters used to calculate the centrifugal forces. The non-dimensional expression of $\overline{Q}_k(\overline{x}_k)$ is:

$$\begin{aligned} Q_k(x) = \left(N_k(x) + \frac{\kappa}{2(1+\nu)} E_k(x) A_k(x) \right) \frac{dW_k}{dx} - \\ \frac{\kappa}{2(1+\nu)} E_k(x) A_k(x) \Psi_k, \end{aligned} \tag{52}$$

where:

$$W_k = \frac{\overline{W}_k}{\overline{L}_k}; \qquad \frac{dW_k}{dx} = \frac{d\overline{W}_k}{d\overline{x}_k}; \qquad \Psi_k = \overline{\Psi}_k, \tag{53}$$

define the non-dimensional displacements . The non-dimensional expression of $\overline{M}_k(\overline{x}_k)$ is:

$$M_k(x) = E_k(x) I_k(x) \frac{d\Psi_k}{dx}, \tag{54}$$

where:

$$\frac{d\Psi_k}{dx} = \overline{L}_k \frac{d\overline{\Psi}_k}{d\overline{x}_k}. \tag{55}$$

The following non-dimensional parameters are defined to calculate the non-dimensional internal forces:

$$N_k(x) = \frac{\overline{N}_k(\overline{x}_k)}{\overline{E}_k(0) \overline{A}_k(0)}; \qquad Q_k(x) = \frac{\overline{Q}_k(\overline{x}_k)}{\overline{E}_k(0) \overline{A}_k(0)}; \qquad M_k(x) = \frac{\overline{M}_k(\overline{x}_k) L_x}{\overline{E}_k(0) \overline{I}_k(0)}. \tag{56}$$

After algebraic manipulation, the non-dimensional expression of differential equation (39) results:

$$c_{k11} \frac{dW_k}{dx} + c_{k12} \frac{d^2 W_k}{dx^2} + c_{k13} \Psi_k + c_{k14} \frac{d\Psi_k}{dx} = \Omega^2 \rho_k(x) A_k(x) W_k, \tag{57}$$

where:

$$\Omega = \sqrt{\frac{\overline{\rho}_1(0) \overline{A}_1(0)}{\overline{E}_1(0) \overline{I}_1(0)}} L^2 \omega, \tag{58}$$

is the frequency coefficient, and the remaining constants in (57) result:

$$
\begin{aligned}
c_{k11} =& -\eta^2\rho_k(x)A_k(x)(R_k+x) - \frac{\kappa}{2(1+\nu)}\frac{s_1^2}{L_k^2}\left(E_k(x)\frac{dA_k(x)}{dx} + \frac{dE_k(x)}{dx}A_k(x)\right);\\
c_{k12} =& -\frac{s_1^2}{L_k^2}N_k(x) - \frac{\kappa}{2(1+\nu)}\frac{s_1^2}{L_k^2}E_k(x)A_k(x);\\
c_{k13} =& -\frac{\kappa}{2(1+\nu)}\frac{s_1^2}{L_k^2}\left(E_k(x)\frac{dA_k(x)}{dx} + \frac{dE_k(x)}{dx}A_k(x)\right);\\
c_{k14} =& \frac{\kappa}{2(1+\nu)}\frac{s_1^2}{L_k^2}E_k(x)A_k(x),
\end{aligned} \tag{59}
$$

and the non-dimensional expression of the differential equation (40) yields:

$$
c_{k21}\frac{dW_k}{dx} + c_{k22}\Psi_k + c_{k23}\frac{d\Psi_k}{dx} + c_{k24}\frac{d^2\Psi_k}{dx^2} = \Omega^2\rho_k(x)I_k(x)\Psi_k, \tag{60}
$$

where:

$$
\begin{aligned}
c_{k21} &= -\frac{\kappa}{2(1+\nu)}s_1^2 s_k^2 E_k(x)A_k(x);\\
c_{k22} &= \frac{\kappa}{2(1+\nu)}s_1^2 s_k^2 E_k(x)A_k(x) - \eta^2\rho_k(x)I_k(x);\\
c_{k23} &= -\frac{s_1^2}{L_k^2}\left(E_k(x)\frac{dI_k(x)}{dx} + \frac{dE_k(x)}{dx}I_k(x)\right);\\
c_{k24} &= -\frac{s_1^2}{L_k^2}E_k(x)I_k(x).
\end{aligned} \tag{61}
$$

The corresponding non-dimensional expressions for compatibility of displacement are obtained from the equations (41) and (42), resulting:

$$
-L_{k-1}W_{k-1}(1) + L_kW_k(0) = 0, \tag{62}
$$

and:

$$
-\Psi_{k-1}(1) + \Psi_k(0) = 0. \tag{63}
$$

The non-dimensional expressions for compatibility of internal forces are obtained from the equations (43) and (44). For $Q_k(x)$ it results:

$$
-\alpha_{E(k-1)}\alpha_{A(k-1)}Q_{k-1}(1) + \alpha_{Ek}\alpha_{Ak}Q_k(0) = 0, \tag{64}
$$

where $Q_{k-1}(1)$ and $Q_k(0)$ are obtained from equation (52), resulting:

$$\begin{aligned} Q_{k-1}(1) = & \left(N_{k-1}(1) + \frac{\kappa}{2(1+\nu)} E_{(k-1)}(1) A_{(k-1)}(1) \right) \frac{dW_{k-1}}{dx}|_{x=1} - \\ & \frac{\kappa}{2(1+\nu)} E_{(k-1)}(1) A_{(k-1)}(1) \Psi_{k-1}|_{x=1}; \\ Q_k(0) = & \left(N_k(0) + \frac{\kappa}{2(1+\nu)} E_k(0) A_k(0) \right) \frac{dW_k}{dx}|_{x=0} - \\ & \frac{\kappa}{2(1+\nu)} E_k(0) A_k(0) \Psi_k|_{x=0}. \end{aligned} \tag{65}$$

For $M_k(x)$ it results:

$$-\frac{\alpha_{E(k-1)}\alpha_{I(k-1)}}{L_{k-1}} M_{k-1}(1) + \frac{\alpha_{Ek}\alpha_{Ik}}{L_k} M_k(0) = 0, \tag{66}$$

where $M_{k-1}(1)$ and $M_k(0)$ are obtained from equation (54), resulting:

$$\begin{aligned} M_{k-1}(1) = & E_{k-1}(1) I_{k-1}(1) \frac{d\Psi_{k-1}}{dx}|_{x=1}; \\ M_k(0) = & E_k(0) I_k(0) \frac{d\Psi_k}{dx}|_{x=0}. \end{aligned} \tag{67}$$

The non-dimensional form of boundary conditions results as follow: In the case of clamped-free boundary conditions, from equations (45) is obtained:

$$W_1|_{x=0} = 0; \qquad \Psi_1|_{x=0} = 0; \qquad Q_d|_{x=1} = 0; \qquad M_d|_{x=1} = 0. \tag{68}$$

In the case of clamped-slider boundary conditions, from equations (46) it results:

$$W_1|_{x=0} = 0; \qquad \Psi_1|_{x=0} = 0; \qquad W_d|_{x=1} = 0; \qquad M_d|_{x=1} = 0. \tag{69}$$

Finally, in the case of clamped-clamped boundary conditions, from equations (47) is yield:

$$W_1|_{x=0} = 0; \qquad \Psi_1|_{x=0} = 0; \qquad W_d|_{x=1} = 0; \qquad \Psi_d|_{x=1} = 0. \tag{70}$$

3.3 Analogous quadrature differential equations

The analogous equation for $N(x)$ is obtained from equation (48):

$$N_{k,i} = \eta^2 \frac{l_k^2}{s_1^2} \left(R_k v_{k,n} + \phi_{k,n} - R_k v_{k,i} - \phi_{k,i} \right) + N_{k+1}, \tag{71}$$

and similarly, the analogous equation for $Q(x)$ is obtained from equation (52):

$$Q_{k,i} = \left(N_{k,i} + \frac{\kappa}{2(1+\nu)} E_{k,i} A_{k,i} \right) \sum_{j=1}^{n} A_{i,j}^{(1)} W_{k,j} - \frac{\kappa}{2(1+\nu)} E_{k,i} A_{k,i} \Psi_{k,i}. \tag{72}$$

The analogous equation for $M(x)$ is obtained from equation (54):

$$M_{k,i} = E_{k,i} I_{k,i} \sum_{j=1}^{n} A_{i,j}^{(1)} \Psi_{k,j}. \tag{73}$$

On the other hand, the analogous equations for the differential equations are obtained from equations (57) and (60):

$$\begin{aligned} & c_{k11,i} \sum_{j=1}^{n} A_{i,j}^{(1)} W_{k,j} + c_{k12,i} \sum_{j=1}^{n} A_{i,j}^{(2)} W_{k,j} \\ & + c_{k13,i} \Psi_{k,i} + c_{k14,i} \sum_{j=1}^{n} A_{i,j}^{(1)} \Psi_{k,j} = \Omega^2 \rho_{k,i} A_{k,i} W_{k,i}, \end{aligned} \tag{74}$$

and:

$$\begin{aligned} & c_{k21,i} \sum_{j=1}^{n} A_{i,j}^{(1)} W_{k,j} + c_{k22,i} \Psi_{k,i} + c_{k23,i} \sum_{j=1}^{n} A_{i,j}^{(1)} \Psi_{k,j} \\ & + c_{k24,i} \sum_{j=1}^{n} A_{i,j}^{(2)} \Psi_{k,j} = \Omega^2 \rho_{k,i} I_{k,i} \Psi_{k,i}, \end{aligned} \tag{75}$$

while, the analogous equations for compatibility equations of displacements are obtained from equations (62) and (63)

$$-L_{k-1} W_{(k-1),n} + L_k W_{k,1} = 0, \tag{76}$$

and:

$$-\Psi_{(k-1),n} + \Psi_{k,1} = 0. \tag{77}$$

For compatibility equations of internal forces, the analogous equation are obtained from equations (64) and (66):

$$\begin{aligned} & -\alpha_{E(k-1)} \alpha_{A(k-1)} \left(N_{(k-1),n} + \frac{\kappa}{2(1+\nu)} E_{(k-1),n} A_{(k-1),n} \right) \sum_{j=1}^{n} A_{n,j}^{(1)} W_{(k-1),j} - \\ & \frac{\kappa}{2(1+\nu)} E_{(k-1),n} A_{(k-1),n} \Psi_{(k-1),n} + \\ & \alpha_{Ek} \alpha_{Ak} \left(N_{k,1} + \frac{\kappa}{2(1+\nu)} E_{k,1} A_{k,1} \right) \sum_{j=1}^{n} A_{1,j}^{(1)} W_{k,j} - \\ & \frac{\kappa}{2(1+\nu)} E_{k,1} A_{k,1} \Psi_{k,1}, \end{aligned} \tag{78}$$

and:

$$\begin{aligned} & -\frac{\alpha_{Ek-1} \alpha_{Ik-1}}{l_{k-1}} E_{(k-1),n} I_{(k-1),n} \sum_{j=1}^{n} A_{n,j}^{(1)} \Psi_{(k-1),j} + \\ & \frac{\alpha_{Ek} \alpha_{Ik}}{l_k} E_{k,1} I_{k,1} \sum_{j=1}^{n} A_{1,j}^{(1)} \Psi_{k,j}. \end{aligned} \tag{79}$$

Finally, the analogous equation for boundary conditions are obtained from equations (68) to (70). In the case of clamped-free boundary conditions, from equations (68) it is obtained:

$$W_{1,1} = 0; \qquad \Psi_{1,1} = 0;$$

$$\left(N_{d,n} + \frac{\kappa}{2(1+\nu)} E_{d,n} A_{d,n} \right) \sum_{j=1}^{n} A^{(1)}_{n,j} W_{d,j} - \frac{\kappa}{2(1+\nu)} E_{d,n} A_{d,n} \Psi_{d,n} = 0; \tag{80}$$

$$\sum_{j=1}^{n} A^{(1)}_{n,j} \Psi_{d,j} = 0.$$

For the case of clamped-slider boundary conditions, from equations (69) it is expressed:

$$W_{1,1} = 0; \qquad \Psi_{1,1} = 0; \qquad W_{d,n} = 0; \qquad \sum_{j=1}^{n} A^{(1)}_{n,j} \Psi_{d,j} = 0, \tag{81}$$

and for the case of clamped-clamped boundary conditions, from equations (70) results in:

$$W_{1,1} = 0; \qquad \Psi_{1,1} = 0; \qquad W_{d,n} = 0; \qquad \Psi_{d,n} = 0. \tag{82}$$

4 NUMERICAL RESULTS AND DISCUSSION

4.1 Convergence analysis of DQM

The appropriate number of nodal points to make the DQM mesh, is obtained by means of a convergence analysis. This analysis is performed by increasing at each step the number of nodal points n. In the present case, the appropriate number of nodal points is achieved if the first five natural frequencies, do not change significantly when does increase the value of n. In Table 1, it can be seen that, 23 nodes are enough to accomplish the stability of the first five natural frequency coefficients. Is important to point out that, for this analysis, an axially functionally graded beam model has been considered. Once the value of n has been obtained, the DQM mesh can be defined, which allows building the differential quadrature analogous equations.

n	Ω_1	Ω_2	Ω_3	Ω_4	Ω_5
5	12.6340	25.2920	39.7171	42.6266	57.3018
7	12.6538	25.3338	37.9450	40.7069	54.1725
9	12.6631	25.3035	37.8692	40.6598	54.0723
11	12.6663	25.2950	37.8353	40.6441	54.0214
13	12.6675	25.2922	37.8233	40.6407	54.0012
15	12.6680	25.2912	37.8188	40.6398	53.9935
17	12.6682	25.2909	37.8171	40.6395	53.9907
19	12.6682	25.2907	37.8165	40.6394	53.9896
21	12.6682	25.2907	37.8162	40.6393	53.9892
23	**12.6683**	**25.2907**	**37.8161**	**40.6393**	**53.9890**
25	12.6683	25.2907	37.8161	40.6393	53.9890

Table 1: Convergence analysis of DQM, for the first natural frequency coefficients Ω_i, in a clamped-free non-homogeneous rotating Timoshenko beam:, $R_0 = 0$; $n_{E1} = 2$; $n_{\rho 1} = 2$; $\eta = 12$; $r_1 = 0.15$; $\nu = 0.3$; $n_{h1} = 1$; $n_{b1} = 1$; $h_B/h_A = 0.5$; $b_B/b_A = 0.5$.

4.2 Characteristics of the models under study

To see the influence, in the dynamic response of the beam, that produce the presence of AFGM, the first five natural frequencies of the beam were calculated in a variety of cases. First, the cases of rotating beam models composed by only one element were analyzed. Then, some cases of rotating beam models composed by two elements, were calculated. These cases have taken into account geometrical and mechanical discontinuities. In all of the cases of beams with inhomogeneous mechanical properties, the materials adopted for the present study have been aluminium and zirconium, which are commonly found in the available technical literature.

4.3 Rotating beam model composed by one element

The particular cases analyed in this section can be grouped in three sets, having each of them, different boundary conditions. In addition, for each group, it has considered some different geometries like the cases of uniform or tapered beams. Figures 5 to 7 show the mesh of models under study. In first place, the clamped-free Timoshenko beams were studied considering different geometries, as it is illustrated in the Figure 5. The main variables that have taken into account were the rotational speed and the slenderness parameters. The corresponding results are shown in the Tables 2 to 4. In some cases, the values obtained by other authors, Rajasekaran (2012), were added at the table to compare results. Is highly remarkable the good agreement between them.

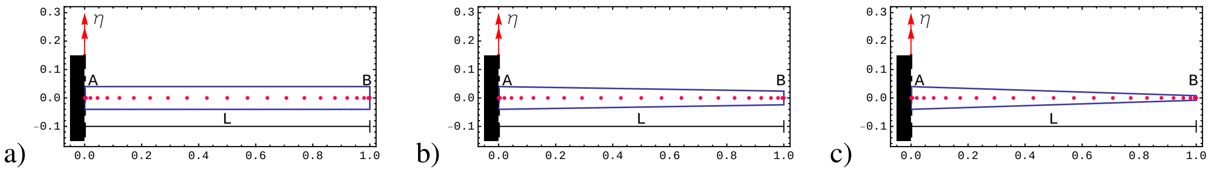

Figure 5: DQM-mesh for clamped-free non-homogeneous rotating Timoshenko beams: $R_0 = 0$; $n_{E1} = 2$; $n_{\rho 1} = 2$; $n_{h1} = 1$; $n_{b1} = 1$: a) $h_B/h_A = b_B/b_A = 1$; b) $h_B/h_A = b_B/b_A = 0.6$; c) $h_B/h_A = b_B/b_A = 0.2$.

η	r	Ω_1	Ω_2	Ω_3	Ω_4	Ω_5
0	0.01	4.28123	23.0665	60.8629	115.896	187.169
	0.08	4.01239	17.0959	36.6134	57.3718	78.3942
	0.15	3.52332	11.6452	23.1527	28.6221	37.1340
5	0.01	6.92170	25.8883	63.7174	118.847	190.202
	0.08	6.54900	20.1594	40.4697	62.1019	83.4267
	0.08	6.5490*	20.1594*	40.4696*	62.1017*	–
	0.15	5.97745	14.9851	27.4302	30.4593	42.2432
12	0.01	13.4798	36.4162	75.7365	131.896	203.945
	0.08	12.7461	30.5335	54.1605	77.9304	93.8777
	0.15	11.6280	20.4731	33.2544	37.0463	51.4733

Table 2: First natural frequency coefficients Ω_i, in a clamped-free non-homogeneous rotating Timoshenko beam: $R_0 = 0$; $n_{E1} = 2$;$n_{\rho 1} = 2$; $n_{h1} = 1$; $n_{b1} = 1$; $\nu = 0.3$; $\kappa = 5/6$; $h_B/h_A = b_B/b_A = 1$. Ref*: Rajasekaran (2012).

η	r	Ω_1	Ω_2	Ω_3	Ω_4	Ω_5
0	0.01	5.17593	20.9855	50.9503	94.8319	152.166
	0.08	4.86359	16.8105	34.3269	54.3130	75.6457
	0.15	4.28301	12.2666	22.9042	33.1773	38.9812
5	0.01	7.63800	23.6977	53.6659	97.5772	154.942
	0.08	7.24768	19.6569	37.6655	58.3131	80.3590
	0.08	7.2477*	19.6569*	37.6655*	58.3131*	–
	0.15	6.61364	15.5588	27.3402	35.8804	42.1169
12	0.01	14.0959	33.7087	65.0116	109.659	167.491
	0.08	13.3514	29.5991	50.3413	73.8215	98.6061
	0.15	12.4578	24.8251	36.4446	39.3076	52.3908

Table 3: First natural frequency coefficients Ω_i, in a clamped-free non-homogeneous rotating Timoshenko beam: $R_0 = 0$; $n_{E1} = 2$; $n_{\rho 1} = 2$; $n_{h1} = 1$; $n_{b1} = 1$; $\nu = 0.3$; $\kappa = 5/6$; $h_B/h_A = b_B/b_A = 0.6$. Ref*: Rajasekaran (2012).

η	r	Ω_1	Ω_2	Ω_3	Ω_4	Ω_5
0	0.01	7.15487	19.2249	39.7377	69.4499	108.396
	0.08	6.71224	16.5976	30.7197	47.8933	67.1292
	0.15	5.88211	13.0263	22.1272	32.6034	43.6898
5	0.01	9.32385	21.8618	42.4294	72.1416	111.082
	0.08	8.81028	19.2358	33.6036	51.0780	70.6807
	0.08	8.8103*	19.2635*	33.6037*	51.0782*	–
	0.15	7.92372	15.9187	25.6954	36.8753	47.0838
12	0.01	15.5354	31.3520	53.3561	83.7435	123.042
	0.08	14.6403	28.4234	44.7996	64.0342	85.4261
	0.15	13.4879	25.3873	37.5863	46.1765	53.5987

Table 4: First natural frequency coefficients Ω_i, in a clamped-free non-homogeneous rotating Timoshenko beam: $R_0 = 0$; $n_{E1} = 2$; $n_{\rho 1} = 2$; $n_{h1} = 1$; $n_{b1} = 1$; $\nu = 0.3$; $\kappa = 5/6$; $h_B/h_A = b_B/b_A = 0.2$. Ref*: Rajasekaran (2012).

Similarly to the case shown before, in Figure 6 are shown the models with pinned-free boundary conditions, with the same cases of geometry shapes.

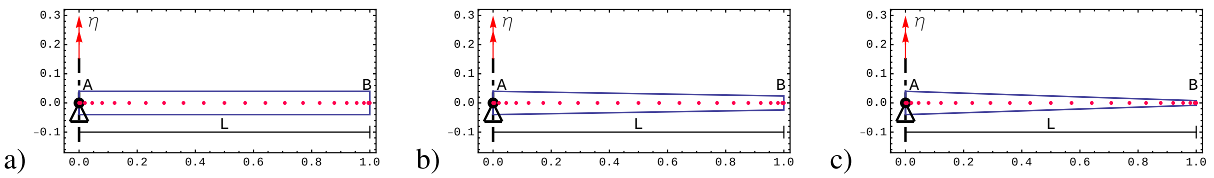

Figure 6: DQM-mesh for pinned-free non-homogeneous rotating Timoshenko beams: $R_0 = 0$; $n_{E1} = 2$; $n_{\rho 1} = 2$; $n_{h1} = 1$; $n_{b1} = 1$: a) $h_B/h_A = b_B/b_A = 1$; b) $h_B/h_A = b_B/b_A = 0.6$; $h_B/h_A = b_B/b_A = 0.2$.

In the Tables 5 to 7 are shown the corresponding results.

η	r	Ω_1	Ω_2	Ω_3	Ω_4	Ω_5
0	0.01	–	16.3316	49.7552	100.855	168.664
	0.08	–	13.8453	34.0090	56.1060	77.5417
	0.15	–	10.7628	22.1493	26.5340	33.0997
5	0.01	4.99819	20.0288	53.1873	104.219	172.017
	0.08	4.88455	17.5728	38.1474	60.9994	82.3463
	0.08	4.8846*	17.5728*	38.1475*	60.9994*	–
	0.15	4.57204	14.4935	24.6886	28.9540	35.5689
12	0.01	11.9957	32.1565	66.9957	118.815	187.069
	0.08	11.7124	28.9691	52.4086	77.6140	88.4994
	0.15	10.3353	20.4620	25.5845	36.7772	42.4267

Table 5: First natural frequency coefficients Ω_i, in a pinned-free non-homogeneous rotating Timoshenko beam: $R_0 = 0$; $n_{E1} = 2$; $n_{\rho 1} = 2$; $n_{h1} = 1$; $n_{b1} = 1$; $\nu = 0.3$; $\kappa = 5/6$; $h_B/h_A = b_B/b_A = 1$. Ref*: Rajasekaran (2012).

η	r	Ω_1	Ω_2	Ω_3	Ω_4	Ω_5
0	0.01	–	14.4757	41.0136	81.6652	136.028
	0.08	–	12.8868	31.0503	52.3053	74.5726
	0.15	–	10.6105	22.0302	29.4930	33.8205
5	0.01	4.99824	17.8931	44.1578	84.7004	139.022
	0.08	4.88817	16.3407	34.6668	56.4371	79.3757
	0.08	4.8882*	16.3408*	34.6669*	56.4372*	–
	0.15	4.59645	14.2349	26.2208	29.5343	38.8578
12	0.01	11.9958	29.0890	56.7495	97.8245	152.438
	0.08	11.7251	27.2536	47.9566	72.3123	96.9886
	0.15	10.6735	23.6563	27.3669	39.1944	43.3993

Table 6: First natural frequency coefficients Ω_i, in a pinned-free non-homogeneous rotating Timoshenko beam: $R_0 = 0$; $n_{E1} = 2$; $n_{\rho 1} = 2$; $n_{h1} = 1$; $n_{b1} = 1$; $\nu = 0.3$; $\kappa = 5/6$; $h_B/h_A = b_B/b_A = 0.6$. Ref*: Rajasekaran (2012).

η	r	Ω_1	Ω_2	Ω_3	Ω_4	Ω_5
0	0.01	–	13.5330	31.8753	59.3879	96.2022
	0.08	–	12.5123	26.9529	45.0843	65.3359
	0.15	–	10.7826	20.9211	31.3525	33.0611
5	0.01	4.99751	16.5901	34.8543	62.2780	99.0359
	0.08	4.84231	15.5704	30.1061	48.4285	68.9872
	0.08	4.8423*	15.5706*	30.1060*	48.4294*	–
	0.15	4.43942	13.9158	24.5450	31.8737	36.8859
12	0.01	11.9940	26.6153	46.4316	74.4814	111.515
	0.08	11.6119	25.3892	41.8885	61.801	84.0335
	0.15	10.2388	22.8060	30.9224	37.6352	52.0501

Table 7: First natural frequency coefficients Ω_i, in a pinned-free non-homogeneous rotating Timoshenko beam: $R_0 = 0$; $n_{E1} = 2$; $n_{\rho 1} = 2$; $n_{h1} = 1$; $n_{b1} = 1$; $\nu = 0.3$; $\kappa = 5/6$; $h_B/h_A = b_B/b_A = 0.2$. Ref*: Rajasekaran (2012).

Finally, in Figure 7 it is shown the model with clamped-slider boundary conditions.

a) b) c)

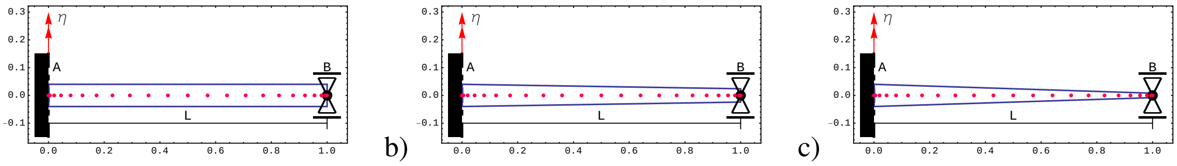

Figure 7: DQM-mesh for clamped-slider non-homogeneous rotating Timoshenko beams: $R_0 = 0$; $n_{E1} = 2$; $n_{\rho 1} = 2$; $n_{h1} = 1$; $n_{b1} = 1$: a) $h_B/h_A = b_B/b_A = 1$; b) $h_B/h_A = b_B/b_A = 0.6$; c) $h_B/h_A = b_B/b_A = 0.2$.

In the Tables 8 to 10 can be seen the corresponding results.

η	r	Ω_1	Ω_2	Ω_3	Ω_4	Ω_5
0	0.01	15.2837	47.9606	98.5686	165.798	248.286
	0.08	12.0899	30.0762	50.9878	72.6812	87.2899
	0.15	8.71520	18.9087	27.3656	30.8337	40.9872
5	0.01	17.0668	50.4722	101.340	168.719	251.315
	0.08	14.0315	33.4671	55.5305	78.1611	87.4356
	0.08	14.0314*	33.4670*	55.5302*	78.1607*	–
	0.15	11.1319	22.8332	27.8573	36.5602	42.2489
12	0.01	23.5572	60.8253	113.489	181.900	265.195
	0.08	20.4756	45.5669	72.1642	85.9581	99.8989
	0.15	17.9458	23.5133	36.9693	40.4257	56.0777

Table 8: First natural frequency coefficients Ω_i, in a clamped-slider non-homogeneous rotating Timoshenko beam: $R_0 = 0$; $n_{E1} = 2$; $n_{\rho 1} = 2$; $n_{h1} = 1$; $n_{b1} = 1$; $\nu = 0.3$; $\kappa = 5/6$; $h_B/h_A = b_B/b_A = 1$. Ref*: Rajasekaran (2012).

η	r	Ω_1	Ω_2	Ω_3	Ω_4	Ω_5
0	0.01	13.2817	39.3903	79.7559	133.763	200.706
	0.08	11.1680	27.5455	47.2409	68.4587	90.4368
	0.15	8.49757	18.3558	29.8230	36.4945	42.2330
5	0.01	14.9712	41.7160	82.2891	136.407	203.424
	0.08	12.9202	30.3725	50.8760	72.9010	95.6753
	0.08	12.9202*	30.3725*	50.8759*	72.9007*	–
	0.15	10.5405	22.0869	34.8795	36.6740	47.8731
12	0.01	21.0350	51.2009	93.3306	148.299	215.861
	0.08	18.8170	40.8701	64.9878	90.3030	113.416
	0.15	16.7538	31.2878	38.0702	44.1624	55.6772

Table 9: First natural frequency coefficients Ω_i, in a clamped-slider non-homogeneous rotating Timoshenko beam: $R_0 = 0$; $n_{E1} = 2$; $n_{\rho 1} = 2$; $n_{h1} = 1$; $n_{b1} = 1$; $\nu = 0.3$; $\kappa = 5/6$; $h_B/h_A = b_B/b_A = 0.6$. Ref*: Rajasekaran (2012).

η	r	Ω_1	Ω_2	Ω_3	Ω_4	Ω_5
0	0.01	10.8673	29.1238	56.5723	93.2747	139.092
	0.08	9.73263	23.2542	40.1305	59.1829	79.6873
	0.15	7.95456	16.9212	27.4116	38.6669	47.6062
5	0.01	12.5015	31.3051	58.9495	95.7501	141.626
	0.08	11.3481	25.5712	42.9053	62.4073	83.3743
	0.08	11.3482*	25.5713*	42.9053*	62.4072*	–
	0.15	9.65305	19.7335	31.1127	43.0685	48.0915
12	0.01	18.1304	39.9196	69.0587	106.692	153.074
	0.08	16.6843	34.2873	54.0337	75.7018	98.7597
	0.15	14.9947	29.2497	42.398	48.4472	59.7818

Table 10: First natural frequency coefficients Ω_i, in a clamped-slider non-homogeneous rotating Timoshenko beam : $R_0 = 0$; $n_{E1} = 2$; $n_{\rho 1} = 2$; $n_{h1} = 1$; $n_{b1} = 1$; $\nu = 0.3$; $\kappa = 5/6$; $h_B/h_A = b_B/b_A = 0.2$. Ref*: Rajasekaran (2012).

4.4 Rotating beam model of two elements

One of the more powerful characteristics of the proposed algorithm is the application in beams composed by multiple elements. In this approach a beam composed by 2 elements is adopted. In Figure 8 can be seen the geometry and the corresponding DQM-mesh of the model under analysis.

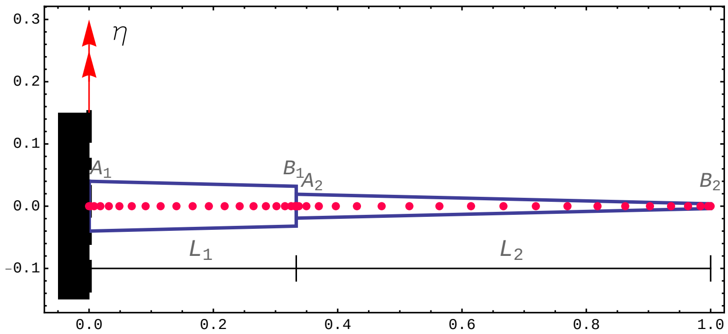

Figure 8: DQM-mesh in a clamped-free non-homogeneous rotating Timoshenko beam, with 2 elements. $R_0 = 0$; $n_{h1} = 1$; $n_{b1} = 1$; $n_{h2} = 1$; $n_{b2} = 1$; $L_1 = 1/3$; $L_2 = 2/3$; $h_{B_1}/h_{A_1} = 0.8$; $h_{B_2}/h_{A_2} = 0.2$; $h_{A_2}/h_{B_1} = 0.6$; $b_{B_1}/b_{A_1} = b_{B_2}/b_{A_2} = b_{A_2}/b_{B_1} = 1$.

Furthermore of the discontinuity in his geometry (see Figure 11), the beam does present discontinuity in the material properties. The first five natural frequency coefficients were calculated. In this particular case were addopted 3 types of materials with uniform, linear and quadratic variation of their material properties laws, along the x axis. The corresponding results can be seen in Table 11.

η	r	*material*	Ω_1	Ω_2	Ω_3	Ω_4	Ω_5
0	0.01	constant	4.00988	12.8130	25.9228	45.9407	75.0967
		linear	4.80255	13.4634	26.0416	45.1780	72.8405
		quadratic	4.69055	13.3175	25.8339	45.1334	73.3634
0	0.08	constant	3.91110	11.6830	22.0409	36.9432	54.6112
		linear	4.65766	12.2442	22.1888	36.4628	53.4411
		quadratic	4.56243	12.1264	21.9702	36.4634	53.7692
0	0.15	constant	3.68627	9.77039	17.3206	27.4527	37.8391
		linear	4.33615	10.2065	17.4871	27.1829	37.2250
		quadratic	4.27439	10.1138	17.2860	27.2112	37.2853
5	0.01	constant	7.51681	17.3322	30.9191	51.4222	80.6642
		linear	7.99731	17.5402	30.5722	50.1678	77.9350
		quadratic	8.08137	17.4026	30.3220	50.0578	78.3412
5	0.08	constant	7.28780	16.0076	27.0297	42.5388	60.3691
		linear	7.73386	16.1263	26.6952	41.5184	58.5965
		quadratic	7.81588	16.0212	26.4835	41.4921	58.8619
5	0.15	constant	6.84281	14.0834	22.8255	33.8634	43.4960
		linear	7.21575	14.0564	22.4188	32.8988	42.4858
		quadratic	7.28792	14.0104	22.3023	32.9297	42.4573
12	0.01	constant	14.4864	29.9778	47.8104	71.6254	102.628
		linear	14.9642	29.2605	46.1526	68.8345	98.2193
		quadratic	14.9575	29.3203	45.9899	68.6025	98.2948
12	0.08	constant	13.8356	27.8329	43.1976	62.0929	81.5385
		linear	14.2417	27.0315	41.5786	59.4360	77.8064
		quadratic	14.2276	27.2099	41.6002	59.4762	78.0615
12	0.15	constant	13.0613	25.8071	39.3669	45.2962	57.0177
		linear	13.3236	24.8330	37.5580	44.8018	54.4574
		quadratic	13.3172	25.1738	37.8203	44.7397	54.6284

Table 11: First natural frequency coefficients Ω_i, in a clamped-free tapered rotating Timoshenko beam with non-homogeneous materials, with 2 elements: $R_0 = 0$; $\nu = 0.3$; $\kappa = 5/6$; $n_{h1} = 1$;$n_{b1} = 1$; $n_{h2} = 1$; $n_{b2} = 1$; $h_{B_1}/h_{A_1} = 0.8$; $h_{B_2}/h_{A_2} = 0.2$; $h_{A_2}/h_{B_1} = 0.6$; $b_{B_1}/b_{A_1} = b_{B_2}/b_{A_2} = b_{A_2}/b_{B_1} = 1$.

5 CONCLUSIONS

The algorithms developed for beams with homogeneous material properties along x-axis have been easily extended for inhomogeneous materials. It can be observed that, the convergence speed for differential quadrature method and the computational effort to obtain the first natural frequencies, does not increase significantly when a lot of new features in the model have been considered. The obtained results for natural frequencies of the beam are in a very good agreement with the reference values obtained from the technical literature. On the other hand, in this approach, the authors have developed an original algorithm, based on the differential quadrature method to calculate a rotating beam model defined with AFGM. The algorithm also takes into account both, discontinuities in the cross section and in material properties. This algorithm proves to be very suitable for solving differential equations with variable coefficients. In Table 1, it is shown excellent accuracy of the results, by defining a quadrature mesh containing a few nodes. The proposed method can be used to solve rotating beams with a wide range of complexities. However, this study does not include the posibility to analyze vibrations out of the plane. Then, a possible future research work, is the torsional vibration analysis and its coupling with transverse vibrations.

Acknowledgement

The authors wish to express their gratitude to the Universidad Nacional del Sur and the Consejo Nacional de Investigaciones Científicas y Técnicas for the financial support which enable this work to be conducted.

REFERENCES

Bambill D., Felix D., and Rossi R. Vibration analysis of rotating timoshenko beams by means of the differential quadrature method. *Journal of Structural Engineering and Mechanics*, 34, 2010.

Banerjee J. Free vibration of centrifugally stiffened uniform and tapered beams using the dynamic stiffness method. *Journal of Sound and Vibration*, 233:857–875, 2000.

Banerjee J. Dynamic stiffness formulation and free vibration analysis of centrifugally stiffened timoshenko beam. *Journal of Sound and Vibration*, 247:97–115, 2001.

Banerjee J., Su H., and Jackson D. Free vibration of rotating tapered beams using the dynamic stiffness method. *Journal of Sound and Vibration*, 298:1034–1054, 2006.

Bellman R. and Casti J. Differential quadrature and long-term integration. *Journal of Math. Anal. App*, 34:235–238, 1971.

Bert C. and Malik M. Differential quadrature method in computational mechanics: A review. *Applied Mechanics Review*, 49:1–28, 1996.

Burden R. and Faires J. *Numerical Analysis*. Brooks/Cole, 2001.

Dumitru I.C. Dynamic modal characteristics of transverse vibrations of cantilevers of parabolic thickness. *Mechanics Research Comunications*, 36:391–404, 2009.

Felix D., Bambill D., and Rossi R. Análisis de vibración libre de una viga timoshenko escalonada, centrífugamente rigidizada, mediante el método de cuadratura diferencial. *Revista Internacional de Métodos Numéricos para Cálculo y Diseño en Ingeniería*, 25, 2009.

Felix D., Rossi R., and Bambill D. Vibraciones transversales por el método de cuadratura diferencial de una viga timoshenko rotante, escalonada y elásticamente vinculada. *Mecánica Computacional*, 27:1957–1973, 2008.

Karami G., Malekzadeh P., and Shahpari S. A dqem for vibration of shear deformable nonuniform beams with general boundary conditions. *Engineering Structures*, 25:1169–1178, 2003.

Lin S. and Hsiao K. Vibration analysis of a rotating timoshenko beam. *Journal of Sound and Vibration*, 240:303–322, 2001.

Petyt M. *Introduction to Finite Element Vibration Analysis*. Cambridge University Press, 1990.

Przemieniecki J.S. *Theory of Matrix Structural Analysis*. McGraw-Hill, Inc., 1968.

Rajasekaran S. Free vibration of centrifugally stiffened axially functionally graded tapered timoshenko beams using differential transformation and quadrature methods. *Applied Mathematical Modelling*, 00:1–24, 2012.

Rossi R. *Introducción al análisis de Vibraciones con el Método de Elementos Finito*. EdiUNS, Universidad Nacional del Sur, Bahía Blanca, Argentina, 2007.

Shu C. and Chen W. On optimal selection of interior points for applying discretized boundary conditions in dq vibration analysis of beams and plates. *Journal of Sound and Vibration*, 222, 1999.

Yaghoobi H. and Fereidoon A. Influence of neutral surface position on deflection of functionally graded beam under uniformly distributed load. *World Applied Sciences Journal*, 10, 2010.